Aerodynamic Characteristics of Scissor-Wing Geometries

Clinton S. Housh,* Bruce P. Selberg,† and Kamran Rokhsaz‡
University of Missouri-Rolla, Rolla, Missouri 65401

A scissor-wing configuration, consisting of two independently sweeping-wing surfaces, is compared with an equivalent fixed-wing geometry baseline over a wide Mach number range. The scissor-wing configuration is shown to have a higher total lift-to-drag ratio than the baseline in the subsonic region primarily due to the slightly higher aspect ratio of the unswept scissor wing. In the transonic region, the scissor wing is shown to have a higher lift-to-drag ratio than the baseline for values of lift coefficient > 0.35. It is also shown that, through the use of wing decalage, the lift of the two independent scissor wings can be equalized. In the supersonic regime, the zero lift wave drag of the scissor wing at maximum sweep is shown to be 50 and 28% less than the zero lift wave drag of the baseline at Mach numbers 1.5 and 3.0, respectively. In addition, a pivot-wing configuration is introduced and compared with the scissor wing. The pivot-wing configuration is shown to have a slightly higher total lift-to-drag ratio than the scissor wing in the supersonic region due to the decreased zero lift wave drag of the pivot-wing configuration.

I. Introduction

THE contradictory requirements for high- and low-speed flight have been a challenge to the aircraft designer since the advent of high-speed flight. Those characteristics that lead to a good low-speed aerodynamic performance manifest themselves as liabilities in the high-speed flight regime. One way to reconcile these differences is through the use of variable wing sweep.

Variable wing sweep has been used successfully over the past 25 years on a variety of aircraft. See, for example, Polhamus and Toll.[1] The basic premise is that the wing is swept at sufficiently high angles in order to keep the leading edge subsonic. With this, the wave drag is reduced in the supersonic flight regime. In the subsonic region, the wing sweep is kept at a minimum for good handling qualities and good aerodynamic performance.

The most familiar variable sweep concept involves sweeping both wings aft. However, with this, a large shift in the aircraft center of pressure results, with a corresponding increase in static margin. This increase in the static margin leads to higher trim drag and reduced maneuverability at high sweep angles.

Oblique wings represent another form of variable sweep. This concept, first introduced by Jones,[2] has had proponents for subsonic, transonic, and supersonic transport configurations, as demonstrated in Refs. 3-5. An oblique wing is hinged on the aircraft center line and skews relative to the fuselage. This antisymmetric geometry leads to a coupling between the longitudinal and lateral modes of the aircraft, which produces rather unacceptable handling qualities.

Rokhsaz[6] and Rokhsaz and Selberg[7] introduced the scissor wing as an alternative to conventional variable sweep designs. In this design, two oblique wings are hinged on the aircraft center line and skew relative to the fuselage. This concept retains geometrical symmetry at all sweep angles.

Rokhsaz and Selberg[7] studied the scissor wing from a stability and control point of view where it was shown that the scissor wing can maintain any desired static margin throughout the Mach number range by judiciously varying the sweep. Given this quality, unacceptably high static margins can be avoided at high sweep angles. Selberg et al.[8] presented some limited aerodynamic performance characteristics of the scissor wing. The purpose of the current paper is to present the results of a comprehensive numerical study of the aerodynamic characteristics of scissor-wing geometries.

Received July 15, 1989; revision received June 21, 1990; second revision received Sept. 8, 1990; accepted for publication Sept. 16, 1990.

*Graduate Student, Aerospace Engineering and Engineering Mechanics; currently, Aerospace Engineer, Naval Weapons Center, China Lake, CA. Student Member AIAA.

†Professor of Mechanical and Aerospace Engineering and Engineering Mechanics. Associate Fellow AIAA.

‡Lecturer, Mechanical and Aerospace Engineering and Engineering Mechanics. Senior Member AIAA.

II. Method of Analysis

A. Aircraft Configurations

For the purpose of comparison, a fixed-wing baseline and a variable sweep scissor-wing configuration were devised and are shown in Fig. 1. Both configurations had a common cone-cylinder fuselage, common horizontal stabilator, and equal total wetted area. The configurations were formulated to represent a typical attack aircraft. The wing area of both configurations is the same, 426 ft^2. The weight of both is set at 50,000 lb giving a wing loading of 117.3 lb/ft^2. The baseline configuration has a leading-edge sweep of 23 deg and an aspect ratio of 3.63. The scissor wing has an aspect ratio of 4.27 in the unswept configuration. The scissor-wing configuration has the same aspect ratio as the baseline at a scissor-wing sweep of 17 deg.

Both configurations were trimmed using only the stabilator, which was placed approximately 66% of the scissor-wing root chord below the wing to avoid geometric interference at high sweep angles. The scissor wing has the added advantage of being able to use wing-mounted elevons for trim at high sweep angles; however, for the purposes of this research, this advantage was not used.

A scissor-wing configuration with a canard instead of a conventional tail was also designed. The canard had the same area as the stabilator and was moved relative to the wing in order to devise a 5% stable configuration and a 9% unstable configuration. The stable canard configuration is shown in Fig. 1f. The wing of the stable canard configuration was moved 60% of the scissor-wing root chord aft to maintain a plausible design. The wing of the unstable canard configuration is at the same location as the conventional designs shown in Fig. 1.

B. Computer Programs

1. *Subsonic and Supersonic Lift and Drag due to Lift*

The lift and drag due to lift in the subsonic and supersonic regimes were predicted using Tulinius's linear vortex lattice method NARUVLE.[9] This method uses the Prandtl-Glauert

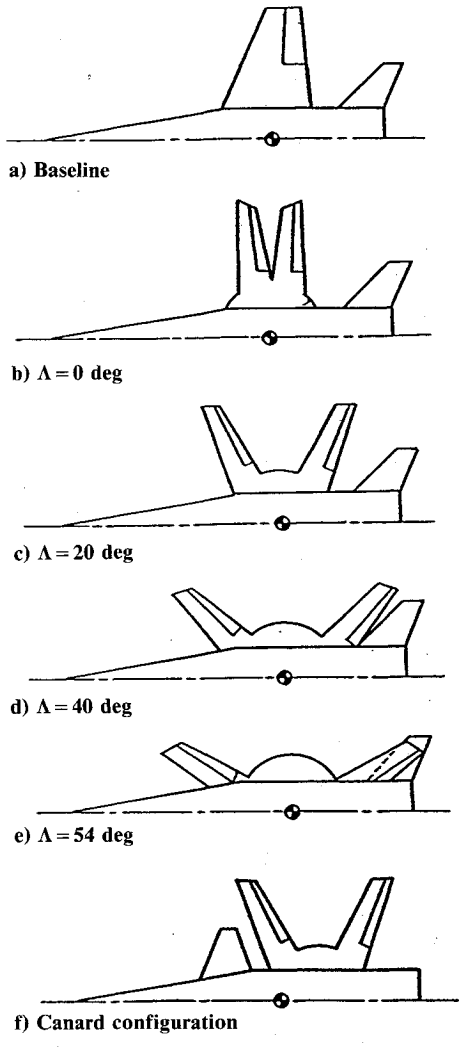

Fig. 1 Aircraft configurations.

transformation in the subsonic regime and supersonic vortices for Mach numbers >1. Being linear, this method is not valid in the transonic region or at high angles of attack.

NARUVLE was compared with the code by Lan and Chang,[10] VORCAM. The two codes were in excellent agreement for values of lift and drag due to lift; however, moment trends were different. NARUVLE was used in this study because of its ability to allow any number of lifting surfaces. This proved invaluable in that modeling the scissor wing requires two wing surfaces, a center section, and a horizontal tail surface. The code was also modified to iteratively trim the aircraft given flight Mach number, wing loading, and dynamic pressure. All results from this code have trim drag included.

NARUVLE was limited to 200 panels, which, in some cases, produced numerical oscillations. Quantitative values may be suspect in some cases; however, the trends are not, and when this code is used to compare two different geometries, firm conclusions may be drawn.

2. Supersonic Zero Lift Wave Drag

The supersonic zero lift wave drag was predicted using the code of Ref. 11, WDRAG2. This code uses Whitcomb's method of area ruling. A convergence study found that 12 azimuthal cutting planes at 70 longitudinal stations assured convergence.

When using WDRAG2, the horizontal tail was modeled using the vertical tails canted 3 deg from the horizontal. This allowed adequate modeling of the wing and center section. The center section and rear wing were modeled as one horizontal surface and the front wing as another horizontal surface. The NACA 64A006 airfoil section was used for the wing surfaces, whereas symmetrical, 4%-thick airfoil was used for the tail. A generic cone-cylinder fuselage was used as a starting point on all of the configurations.

3. Component Buildup Method of Drag Estimation

The component buildup method of drag estimation was used to determine the total drag coefficient in the subsonic and supersonic regimes. The drag due to lift was given by NARUVLE, the supersonic zero lift wave drag by WDRAG2, and the viscous drag by the methods of Nicolai.[12] The viscous drag of the fuselage was determined as a function of Reynolds number, whereas the viscous drag of the wing was taken to be a constant, 0.006, based on the reference wing area of 426 ft^2.

4. Transonic Flow

Transonic analysis of the scissor wing was accomplished through the use of CANTATA.[13] This code uses a finite difference solution to the three-dimensional transonic small perturbation equation. Viscous effects are included through the use of a strip boundary-layer method.

CANTATA can only handle two lifting surfaces. Since the scissor-wing configuration requires two lifting surfaces for the wing, no horizontal tail could be modeled; thus, all CANTATA results are untrimmed. Also, numerical problems resulted when the two wings were put in the same, or close to the same, plane. In order to obtain numerically stable results, a vertical gap of approximately 20% of the root chord of the scissor wing separated the two wings. Because of the two facts mentioned earlier, it could be argued that CANTATA is not capable of modeling the scissor-wing configuration; however, this is not the case. The results from CANTATA may not be directly compatible with the configurations shown in Fig. 1; however, the model used in CANTATA is another possible geometry of the scissor wing. Moreover, CANTATA was used in order to determine if any unusual problems occurred in the transonic region with the basic scissor-wing configuration.

The CANTATA cases were run with and without a fuselage. The cases run with a fuselage are used to show the general trends of this configuration in the transonic region. The cases without a fuselage are used to show detailed wing results.

III. Results

A. Subsonic

The results in this section show the ratio of lift coefficient to drag coefficient vs Mach number, with the drag coefficient being made up of induced drag, wave drag due to lift, and a constant viscous term used to simulate the viscous drag of the wing. The viscous drag of the fuselage and the supersonic zero lift wave drag are not included. Recall also that NARUVLE was limited to the linear range of aerodynamics; thus, the transonic region is an interpolation between the subsonic and supersonic regimes. All cases in this section were trimmed.

Figure 2 shows the lift-to-drag ratio vs Mach number at sea level for the baseline and the scissor-wing configurations at various sweep angles. Two important characteristics are observed.

First, in the subsonic region, the unswept scissor-wing configuration shows a higher lift-to-drag ratio than the baseline. This is due to the slightly higher aspect ratio of the unswept scissor-wing configuration over the baseline. Recall that the aspect ratio for the unswept scissor wing was 4.27, compared with 3.63 for the baseline. The 20-deg sweep scissor-wing case shows a slightly lower lift-to-drag ratio than the baseline. This again shows the effect of the aspect ratio, as the aspect ratio of the 20-deg scissor-wing configuration is 3.1, slightly lower than the baseline's 3.63. The lift-to-drag ratio for the 40- and 54-deg sweep scissor-wing configurations are lower than the baseline and the unswept and the 20-deg scissor-wing cases, again due to the much lower aspect ratio of these configurations.

The other important characteristic is that, in the supersonic region, the ratio of lift to drag is the same, or very nearly the same, for all configurations. Recall that in this figure the viscous drag of the fuselage and the supersonic zero lift wave drag were not included. This figure, then, shows the strong influence that the zero lift wave drag will have on the overall total lift-to-drag ratio of these configurations in the supersonic regime.

Because of the strong influence of the aspect ratio, as discussed earlier, a parametric study of the effect of varying the aspect ratio of the scissor wing was carried out. By holding the total wing area constant, the aspect ratio of the front wing of the scissor wing was increased with a corresponding decrease in the aspect ratio of the rear wing. This was accomplished, first, by holding the chord of the two wings constant and increasing the span of the front wing and decreasing the span of the rear wing; and second, by holding the span of the two wings constant and decreasing the chord of the front wing and increasing the chord of the rear wing. Figure 3 shows the effect of varying the aspect ratio of the scissor-wing configuration by varying the span. As seen in the figure, the higher the aspect ratio of the front wing, the higher the lift-to-drag ratio. The same results would be expected if the aspect ratio of the rear wing was increased instead of increasing the aspect ratio of the front wing. Figure 4 shows the effect of varying the aspect ratio by varying the chord. Little effect is seen. If anything, by changing the aspect ratio with chord, a lower lift-to-drag ratio is seen. In both figures, the same general trends are seen regardless of sweep angle.

Scissor-wing canard configurations were also studied. Figure 5 shows the lift-to-drag ratio vs Mach number for the 9% unstable canard scissor-wing configuration and the 9% unstable conventional tail scissor-wing configuration for both 0- and 20-deg sweep. The figure shows a slight increase in lift-to-drag ratio of the unstable canard configuration over the unstable conventional tail configuration in the unswept condition. At 20-deg sweep, little or no difference is seen between the unstable canard and the unstable conventional tail cases. Figure 6 shows the 5% stable scissor-wing configuration with both a canard and a conventional tail. A marked decrease in lift-to-drag ratio of the canard case relative to the conventional tail in the unswept condition is seen. At 20-deg sweep, little difference is seen between the canard and conventional tail configurations.

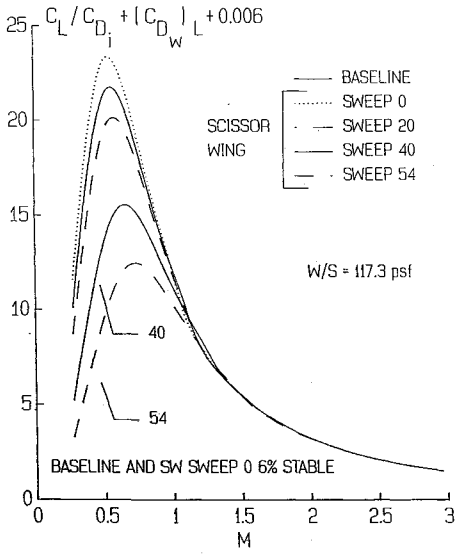

Fig. 2 Lift-to-drag ratio for equal aspect ratios.

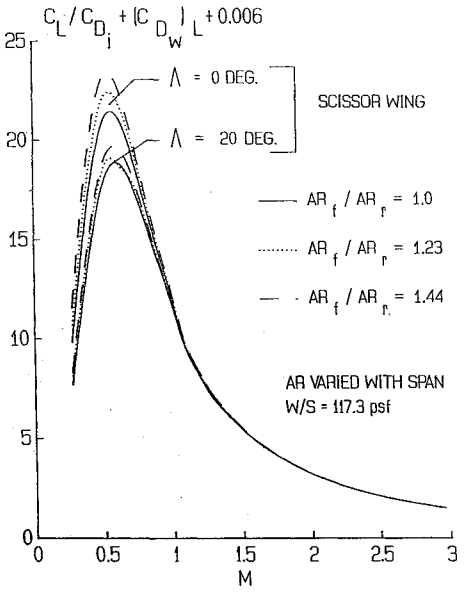

Fig. 3 Effect of span variation on lift-to-drag ratio.

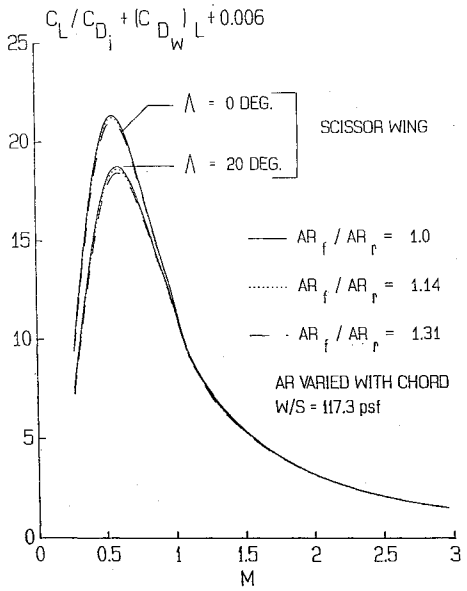

Fig. 4 Effect of chord variation on lift-to-drag ratio.

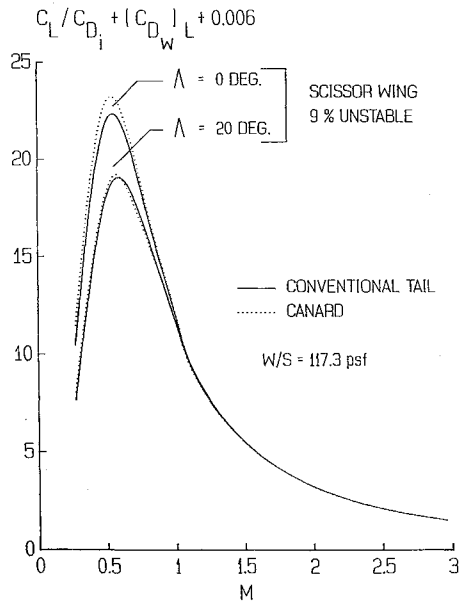

Fig. 5 9% unstable conventional and canard scissor wings.

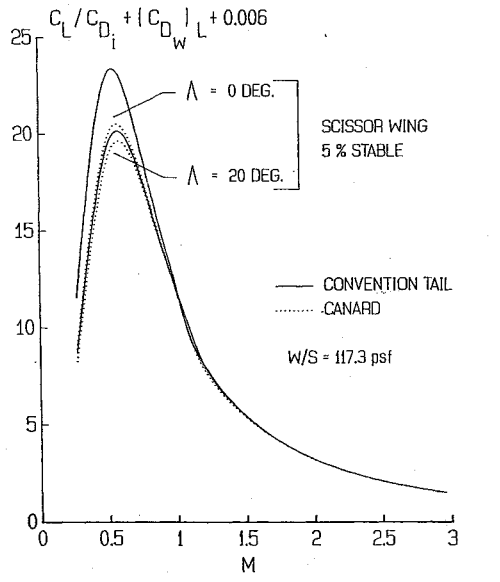

Fig. 6 5% stable conventional and canard scissor wings.

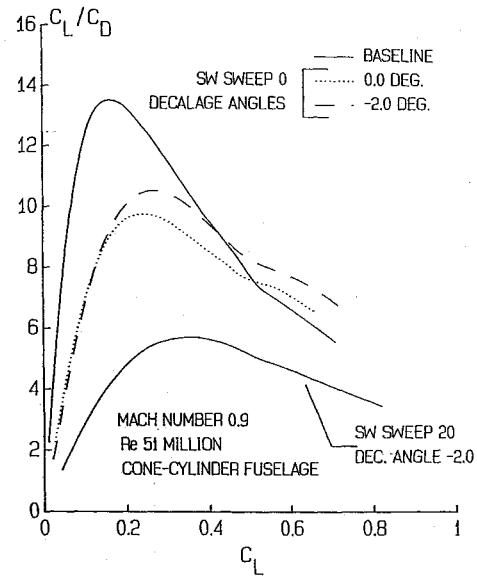

Fig. 8 Lift-to-drag ratio at $M = 0.9$.

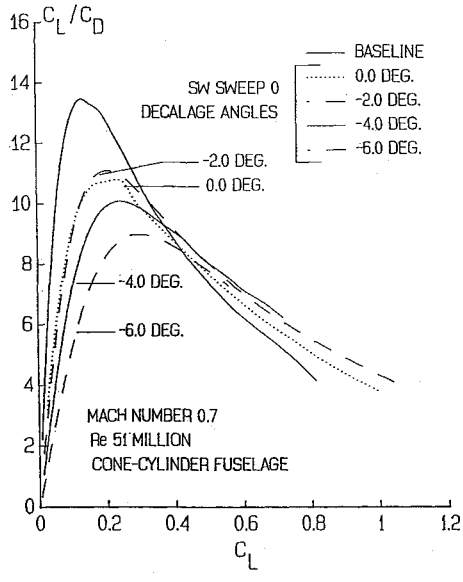

Fig. 7 Effect of decalage on transonic lift-to-drag ratio.

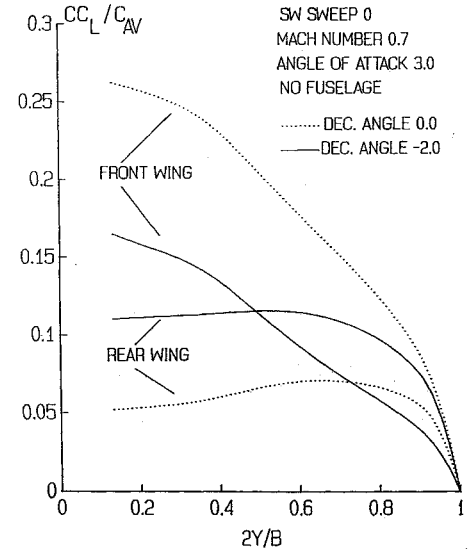

Fig. 9 Effect of decalage on relative lifts.

B. Transonic

The results in this section were obtained from the code CANTATA. Since CANTATA could only handle two surfaces, all results are untrimmed. Also, the configuration used is slightly different from those depicted in Fig. 1. The difference is that there is no center section and the two wings are separated by a gap of approximately 20% of the scissor-wing root chord.

Figure 7 shows the total lift-to-drag ratio vs lift coefficient for the baseline and the unswept scissor-wing configuration at different decalage angles at Mach 0.7. The decalage angle is the relative angle between the two wings. As seen in the figure, a decalage angle of -2.0 deg represents the best compromise for maximum lift to drag over the range of lift coefficients. Figure 8 shows the lift-to-drag ratio vs lift coefficient at a Mach number of 0.9. It is seen that, as the Mach number increases, the increase in lift-to-drag ratio with decalage becomes greater. Figure 8 also shows the 20-deg sweep scissor-wing configuration with a decalage of -2.0 deg. A significant decrease in lift-to-drag is seen for the 20-deg sweep case over the unswept scissor-wing configuration.

In Figs. 7 and 8, the baseline had a higher lift-to-drag ratio than the scissor-wing configuration for lift coefficients less than approximately 0.35. However, for a wing loading of 117.3 lb/ft^2, this range of lift coefficient corresponds only to transonic level flight at low altitude. At a Mach number of 0.8, for these configurations, the trimmed lift coefficient is 0.413 at 30,000 ft. Also, while maneuvering, the average lift coefficient is much greater due to increased load factor. Because of these reasons, the apparent first glance superiority of the baseline over the scissor-wing configuration in the transonic region is not realized.

Figure 9 shows the effect of decalage on the spanwise lift distribution of the unswept scissor-wing configuration without a fuselage. The figure shows the equalizing effect decalage has on the lift of the front and rear wings. Without decalage, nearly all of the configuration lift is produced by the front wing. With -2.0-deg decalage, the lift produced by each wing is nearly the same. As the trimmed lift coefficient increases, the required amount of decalage to equalize the loads carried by the two wings increases. One way to effectively change the decalage of the scissor-wing configuration is to have a leading-edge flap on the front wing and a trailing-edge flap on the rear wing. These flaps can be deflected to simulate the effect of decalage.

Figure 10 shows the moment coefficient vs lift coefficient of the baseline and the unswept scissor-wing configuration at Mach numbers of 0.7, 0.8, and 0.9. Since the magnitude of the moment coefficient depends on the location of the moment center, the actual magnitude of this parameter in Fig. 10 is of no importance. However, the change in slope of the moment coefficient as lift coefficient changes is important. Large changes in the slope can cause control problems. As seen in the figure, the baseline has no effective change in moment slope as the lift varies. However, the unswept scissor wing has a significant change in slope at a Mach number of 0.9.

Figure 11 shows the moment coefficient vs lift coefficient for the baseline, unswept scissor wing, and the 20-deg scissor-wing configurations at a Mach number of 0.9. This figure

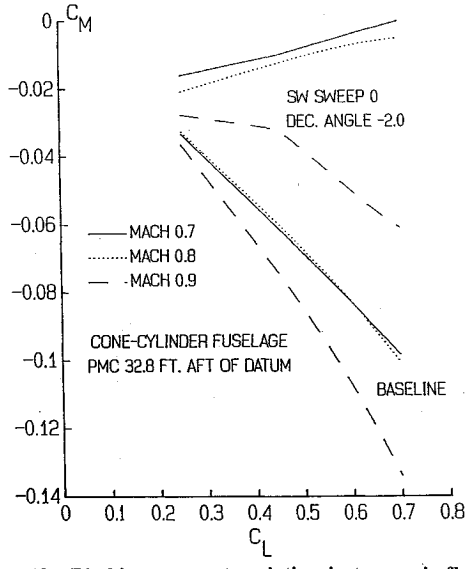

Fig. 10 Pitching moment variation in transonic flow.

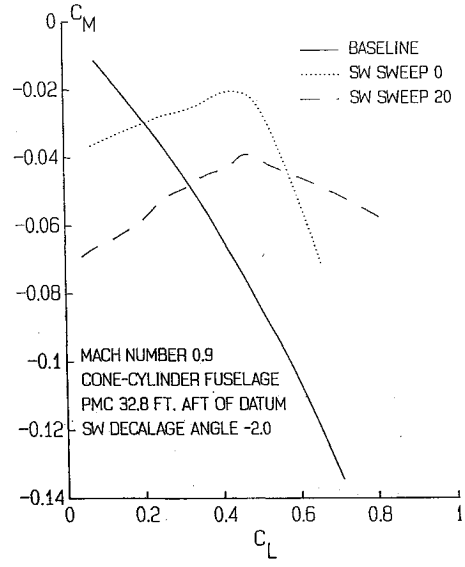

Fig. 11 Pitching moment variation at $M = 0.9$.

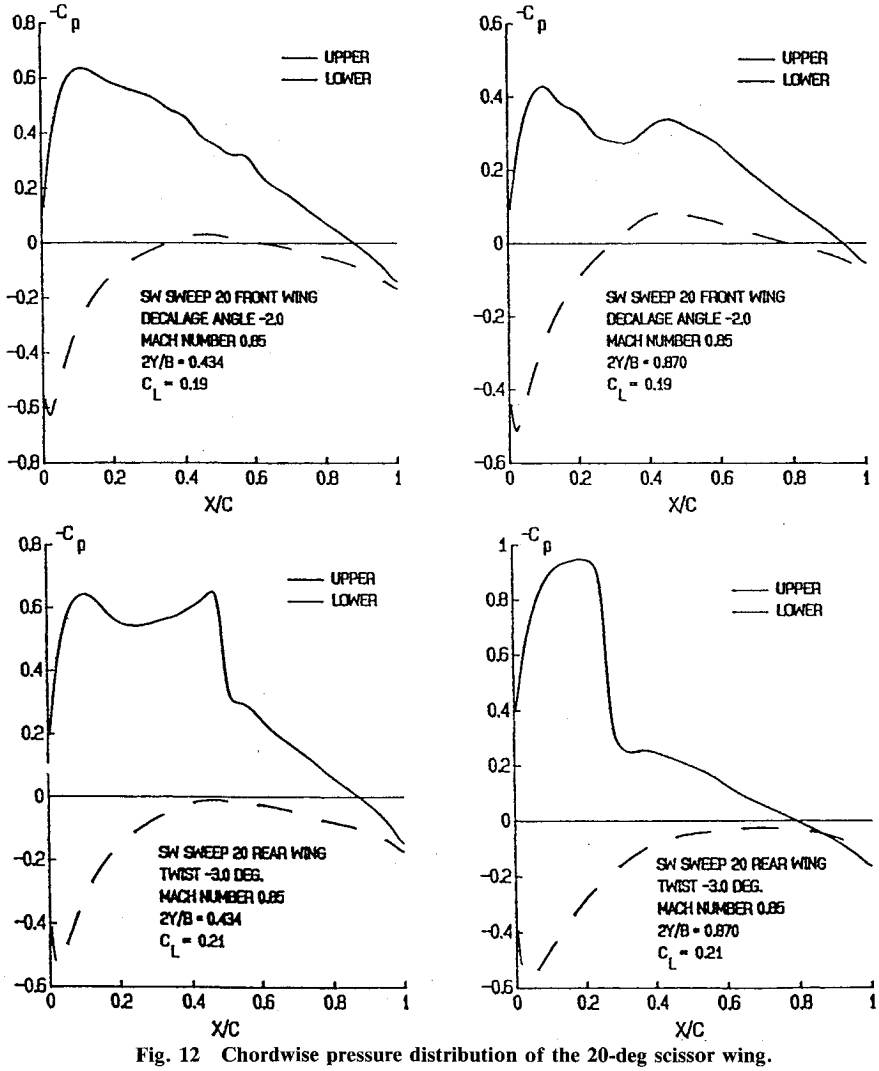

Fig. 12 Chordwise pressure distribution of the 20-deg scissor wing.

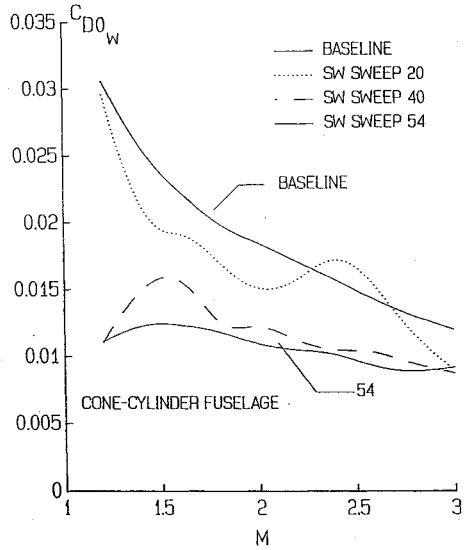

Fig. 13 Zero lift wave drag of the baseline and scissor wing.

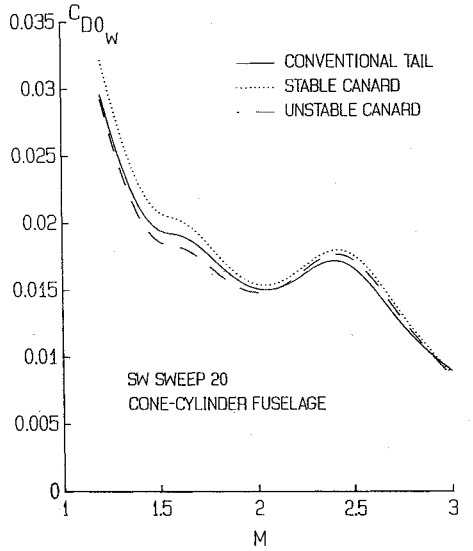

Fig. 14 Zero lift wave drag of conventional and canard scissor wings.

shows the effect that sweeping the scissor-wing configuration has on the slope of the moment. As seen in the figure, by sweeping the scissor-wing configuration, the relative change in moment slope is reduced. This is a strong argument for sweeping the scissor wing at large transonic Mach numbers regardless of the lift-to-drag ratio.

Studies were conducted to optimize the scissor-wing configuration using wing twist. The best results were obtained when the rear wing of the scissor wing was given a washout of 3 deg. Figure 12 shows detailed pressure coefficient plots of the 20-deg scissor wing at a Mach number of 0.85 with 3-deg washout on the rear wing. Plots for both the front wing and the rear wing at two spanwise locations are shown in the figure. Strong shocks are present on the rear wing because the lift coefficient is higher on the rear wing than on the front. These strong shocks are most likely causing the changes in the moment slopes in Figs. 10 and 11 for the Mach 0.9 cases. The strong coupling effect of the two wings is noticed by the fact that, for the unswept scissor wing at the same total lift coefficient, the front wing had a higher lift coefficient than the rear. As the wings are swept apart, the coupling effect decreases and, as is noticed in the figures, the lift becomes greater on the rear wing.

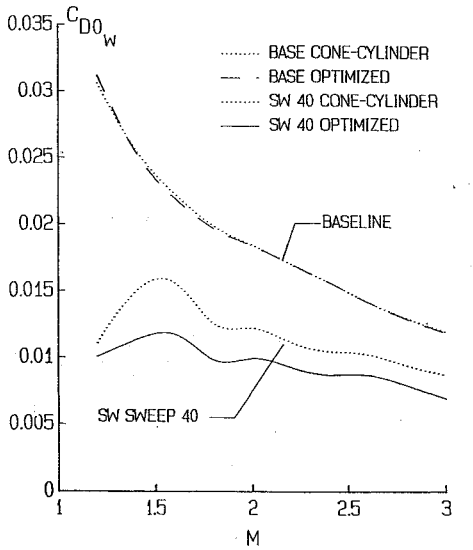

Fig. 15 Effect of fuselage tapering on zero lift wave drag.

C. Supersonic

It was postulated, in the preceding subsonic section, that the zero lift wave drag will be the dominant factor in the total lift-to-drag ratio at supersonic Mach number. This section gives the results of a study of the zero lift wave drag of the scissor-wing configuration as predicted by the code WDRAG2.

Figure 13 shows zero lift wave drag vs Mach number for the baseline and the scissor-wing configuration at various sweep angles. Both configurations had a generic cone-cylinder fuselage and used the NACA 64A006 wing airfoil section. The tail was modeled with a 4%-thick symmetrical airfoil. As seen in the figure, the 54-deg sweep scissor-wing configuration offers a substantial reduction in zero lift wave drag over the baseline; 50 and 28% at Mach numbers 1.5 and 3.0, respectively.

Figure 14 shows the effect of the canard configurations, as discussed earlier, on the zero lift wave drag. Of course, the only effect a canard as opposed to a conventional tail will have on the zero lift wave drag will be on the cross-sectional area distribution. The figure shows that the stable canard configuration has slightly higher zero lift wave drag than the conventional tail configuration and the unstable canard configuration has slightly lower wave drag than the conventional configuration. The differences between all three are very small.

Figure 15 shows the effect of optimizing, that is, area ruling the fuselage to reduce the zero lift wave drag. The figure shows the baseline and the 40-deg scissor-wing configuration with a cone-cylinder fuselage and with an optimized fuselage. The optimized fuselage of both configurations maintained the same volume. The baseline configuration was optimized at a Mach number of 1.5. It is seen in the figure that a cone-cylinder fuselage is near optimum for the baseline throughout the Mach number range. The 40-deg scissor-wing configuration was also optimized at a Mach number of 1.5 and shows a considerable reduction in the zero lift wave drag, ~17% throughout the Mach number range.

Using the optimized baseline fuselage and the optimized scissor-wing fuselage as discussed previously, the total lift-to-drag ratio of the baseline and the scissor-wing configuration at various sweep angles was calculated using the component buildup method of drag estimation. Figure 16 shows the total lift-to-drag ratio as a function of Mach number at an altitude of 30,000 ft. The transonic region is an interpolation between the subsonic and supersonic regimes. As seen in the figure, the scissor wing offers a higher lift-to-drag ratio throughout the Mach number range. In the subsonic region, this increase in lift to drag is due to the slightly higher aspect ratio of the

unswept scissor wing over the baseline. In the supersonic region, the increase in lift to drag is due to the substantial savings in zero lift wave drag of the scissor-wing configuration over the baseline. This increase in lift-to-drag ratio allows the scissor-wing configuration to fly farther and faster than the baseline with equal thrust. For example, using the Breguet range equation for jet aircraft, the 54-deg sweep scissor-wing configuration will have 25% greater range than the baseline at Mach 2.0, 30,000 ft.

D. Pivot Wing

As presently configured, the scissor-wing configuration has a maximum sweep angle of 54 deg. Larger sweep angles, around 70 deg, could be achieved if the unswept configuration had a leading-edge sweep around 15 deg. With leading-edge sweep in the unswept position, low-speed subsonic performance will be sacrificed. An alternate approach is a configuration in which four independent wings sweep about outboard pivots much like the present variable sweep designs. Such a configuration was devised and called the pivot-wing configuration and is shown in Fig. 17. This configuration was studied using both NARUVLE and WDRAG2.

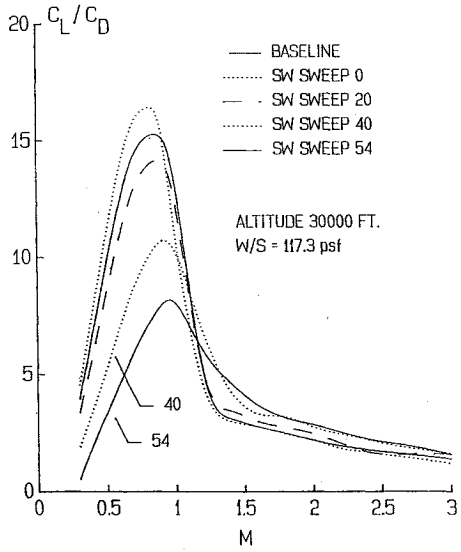

Fig. 16 Total configuration lift-to-drag ratio.

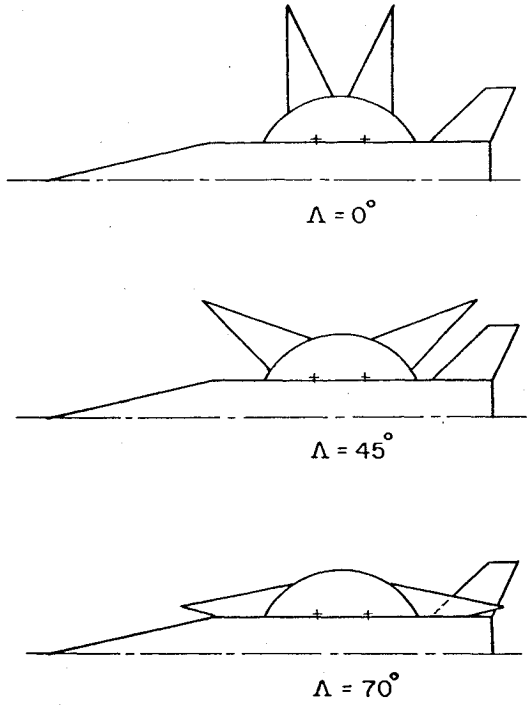

Fig. 17 Pivot-wing configurations.

The pivot-wing configuration has triangular wing planforms because wave drag studies comparing triangular with trapezoidal wing planforms demonstrated that, at Mach 1.5, triangular wings reduced the zero lift wave drag by approximately 26% over trapezoidal wings. At Mach 2.5, the triangular wings reduced the zero lift wave drag by approximately 10%. One disadvantage of using triangular wings is that tip stall problems may occur. This problem was neglected in this study.

Figure 18 shows the effect of optimizing the pivot-wing configuration by area ruling the fuselage. The 70-deg pivot-wing configuration was optimized at a Mach number of 3.0. Slight reductions in zero lift wave drag are seen using the optimized fuselage over the cone-cylinder fuselage. The 70-deg sweep pivot wing offers substantial savings in zero lift wave drag over the baseline. Using the optimized configurations, a reduction in wave drag is seen on the order of 60 and 36% at Mach numbers 1.5 and 3.0, respectively.

Figure 19 shows the total lift-to-drag ratio of the pivot-wing configuration using the component buildup method of drag estimation. The transonic region is an interpolation between the subsonic and supersonic regions. This figure should be

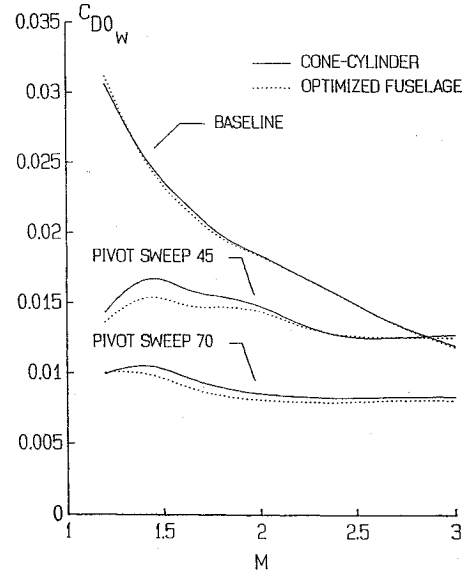

Fig. 18 Effect of fuselage tapering on pivot wing zero lift wave drag.

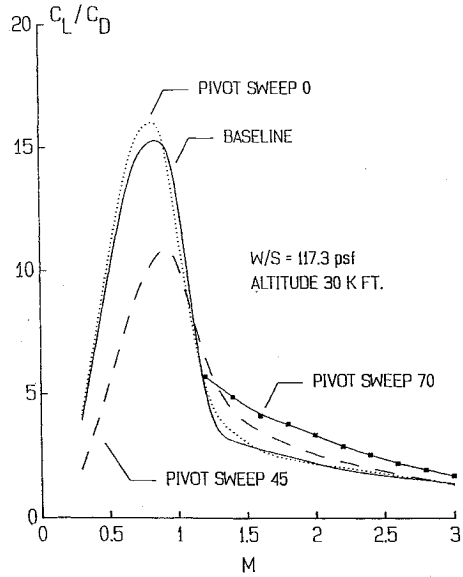

Fig. 19 Total pivot-wing configuration lift-to-drag ratio.

compared with Fig. 16. Throughout the subsonic region, the pivot wing offers no advantage over the scissor-wing configuration. In the supersonic regime, due to the slightly lower zero lift wave drag of the 70-deg sweep pivot wing over the 54-deg sweep scissor wing, the total lift to drag of the pivot wing is slightly higher than the total lift to drag of the scissor wing: 12.9 and 7.1% higher at Mach numbers 1.6 and 3.0, respectively.

As shown earlier, the pivot wing offers a slight aerodynamic benefit, $<13\%$, over the scissor-wing configuration. An additional advantage of the pivot wing is the ability of this configuration to sweep the front and rear wings at different rates. Thus, for example, the front wings could be swept at a larger angle than the rear wings. The benefits of this advantage have not been fully explored at the time of this writing. Additional work is being done in this direction.

IV. Conclusions

The scissor-wing configuration with two independently sweeping wing surfaces was compared with an equivalent fixed wing geometry baseline. In addition, a pivot-wing configuration was introduced and compared with the scissor wing. The following conclusions were drawn.

1) The scissor-wing configuration has a higher total lift-to-drag ratio than the baseline in the subsonic region due to the slightly higher aspect ratio of the unswept scissor wing.

2) In the transonic region, the scissor wing has a higher total lift-to-drag ratio than the baseline for lift coefficients >0.35.

3) The lift of the independent scissor wings can be equalized through the use of wing decalage.

4) The scissor-wing configuration has much lower zero lift wave drag than the baseline: 50 and 28% at Mach numbers 1.5 and 3.0, respectively.

5) The pivot-wing configuration, with its greater sweep angles and triangular wings, has lower zero lift wave drag than the scissor-wing configuration: 10 and 8% at Mach numbers 1.5 and 3.0, respectively.

6) The reduction in zero lift wave drag results in an increase in lift to drag allowing the scissor-wing configuration and the pivot-wing configuration to fly farther and faster than the baseline with equal thrust and weight.

Acknowledgments

This research was sponsored by NASA Langley Research Center under Grant NAG-1-975. Percy Bobbitt and William Henderson were the contract monitors.

References

[1]Polhamus, E. C., and Toll, T. A., "Research Related to Variable Sweep Aircraft Development," NASA TM-83121, May 1981.

[2]Jones, R. T., "Oblique-Wing Supersonic Aircraft," United States Patent #3,971,535, 1976.

[3]Bradley, E. S., Honrath, J., Tomlin, K. H., Swift, G., Shumpert, P., and Warnock, W., "An Analytical Study for a Subsonic Oblique Wing Transport Concept, NASA CR-137896, July 1976.

[4]Anon., "Oblique Wing Transonic Transport Configuration Development," Dept. of Preliminary Design, Boeing Commercial Airplane Co., NASA CR-151928, Jan. 1977.

[5]Van der Velden, A. J. M., and Torenbeek, E., "Design of a Small Supersonic Oblique-Wing Transport Aircraft," *Journal of Aircraft*, Vol. 26, No. 3, 1989, pp. 193–197.

[6]Rokhsaz, K., "Scissor Wing, Patent Disclosure," Univ. of Missouri Patents and Licensing Office, Columbia, MO, UMR Disclosure #87-UMR-023, 1986.

[7]Rokhsaz, K., and Selberg, B. P., "Static Stability and Control Characteristics of Scissor Wing Configurations," *Journal of Aircraft*, Vol. 27, No. 4, 1990, pp. 294–299.

[8]Selberg, B. P., Rokhsaz, K., and Housh, C. S., "Some Aerodynamic Characteristics of the Scissor Wing Configuration," Society of Automotive Engineers Paper 892202, Sept. 1989.

[9]Tulinius, J., "Unified Subsonic, Transonic, and Supersonic NAR Vortex Lattice," North American Rockwell, Los Angeles, CA, TFD-72-523, April 1972.

[10]Lan, E. C., and Chang, J., "Calculation of Vortex Lift Effect for Cambered Wings by the Suction Analogy," NASA CR-3449, July 1981.

[11]Craidon, C. B., "Users' Guide for a Computer Program for Calculating the Zero-Lift Wave Drag of Complex Configurations," NASA TM-85670, Sept. 1970.

[12]Nicolai, L. M., *Fundamentals of Aircraft Design*, 1st ed., Mets, Inc., San Jose, CA, 1975, Chap. 11.

[13]Aidala, P., "Canard/Tail Transonic Analysis," Air Force Wright Aeronautical Laboratories, Wright-Patterson Air Force Base, OH, TR-85-3087, Oct. 1985.